Ferrocene-Containing Chelating Ligands. 1. Solution Study, Synthesis, Crystal Structure, and Electronic Properties of Bis{*N*,*N*′-Ethylenebis((ferrocenylmethyl)amine)}copper(II) Nitrate

Angel Benito,[1a] Juan Cano,[1a] Ramón Martínez-Máñez,*[,1a] Juan Soto,[1a] Jorge Payá,[1a] Francesc Lloret,*[,1b] Miguel Julve,[1b] Juan Faus,[1b] and M. Dolores Marcos[1b]

Departamento de Química y de Ingeniería de la Construcción de la Universidad Politécnica de València, Camino de Vera s/n, 46071 València, Spain, and Departament de Química Inorgànica, Facultat de Química de la Universitat de València, Dr. Moliner 50, 46100 Burjassot (València), Spain

Received June 22, 1992

The synthesis of the Schiff base *N*,*N*′-ethylenebis((ferrocenylmethylidene)amine), $(\eta^5\text{-}C_5H_5)Fe[(\eta^5\text{-}C_5H_4)CH{=}N\text{-}(CH_2)_2N{=}CH(\eta^5\text{-}C_5H_4)]Fe(\eta^5\text{-}C_5H_5)$ (**1**), its parent amine $(\eta^5\text{-}C_5H_5)Fe[(\eta^5\text{-}C_5H_4)CH_2NH(CH_2)_2NHCH_2(\eta^5\text{-}C_5H_4)]Fe(\eta^5\text{-}C_5H_5)$, Fc_2L (**2**), and the complex $[Cu(Fc_2L)_2(NO_3)_2]\cdot 2CH_3OH$ (**3**) are reported. The protonation of **2** and its complex formation with copper(II) have been investigated by potentiometry in dimethyl sulfoxide (dmso)–water (80:20 w/w) mixtures at 25 °C and 0.1 mol dm^{-3} $KClO_4$. The molecular structure of **3** has been determined by single-crystal X-ray analysis. It crystallizes in the triclinic system, space group $P\bar{1}$, a = 7.520(1) Å, b = 11.047(2) Å, c = 16.186(5) Å, α = 101.93(2)°, β = 97.24(2)°, γ = 104.95(1)°, Z = 1, and V = 1247.9(5) Å^3. Refinement of the atomic parameters by least-squares techniques gave a final R factor of 0.046 (R_w = 0.051) for 2941 unique reflections having $I > 2.5\sigma(I)$. The structure of **3** consists in discrete $[Cu(Fc_2L)_2(NO_3)_2]$ neutral units in which the copper(II) ion exhibits a distorted octahedral environment: the four equatorial positions are occupied by the nitrogen atoms of the bidentate ligand, Fc_2L, whereas the apical sites are filled by oxygen atoms of weakly coordinated nitrate anions. **3** is actually a pentanuclear complex with four ferrocene groups which oxidize at the same potential as shown by cyclic voltammetry. So, this compound is a four-electron reservoir potentially capable of acting as a multielectron mediator in redox catalytic reactions. Its electronic properties have been characterized by spectroscopic techniques and variable-temperature magnetic susceptibility measurements.

Introduction

From a redox viewpoint, ferrocene derivatives[2,3] are interesting monoelectron reservoir complexes[4] capable of acting as mediators in redox-catalytic reactions.[5] An important challenge in this field is the design and synthesis of multielectron redox mediators[6] which could transfer several electrons simultaneously at the same potential. The pursued goal is to enhance the efficiency of the redox mediation avoiding high energy pathways which are involved in single-electron reductions. For instance, a two-electron pathway is required to avoid the intermediacy of the H• radical for the formation of H_2 from the photosplitting of water.[7] At this regard, the design of stable species containing several ferrocene groups would be an approach to multielectronic mediators. Each of these active redox centers should then be far enough from one another to have the same redox potential and still close enough to provide all the electrons at the substrate site.

The strategy (molecular engineering) that we have used to achieve it implies the functionalization of ferrocene to yield ferrocenecarboxaldehyde[8] (or ferrocenylamine[9,10]) and its incorporation in the skeleton of classical chelating groups (e.g. polyamines) which are able to coordinate metal ions.[3b,11,12] On the other hand, the occurrence of a metal ion (Lewis acid) and multiple ferrocene units (redox-active centers) in these systems makes them good candidates as redox-catalytic systems capable of promoting redox reactions on a guest substrate through a combination of guest inclusion and subsequent Lewis-acid catalytic activation.[3g] Moreover, one can take advantage of the presence of multiple redox-active centers in them to prepare a great variety of donor (ferrocene)–acceptor (TCNQ, TCNE, ...) electron transfer salts with novel conductivity and magnetic properties.[13]

Our interest in this subject led us to synthesize ferrocene-containing chelating ligands and to explore their complex formation with metal ions in order to set the basis to investigate further their interactions with planar acceptors as well as the magnetic exchange between ferrocenium radicals and paramagnetic metal ions in the corresponding ferrocene-containing metal complexes. In the present paper, we report the synthesis and

(1) (a) Universidad Politécnica de Valencia. (b) Universitat de València.
(2) (a) *Gmelin Handbuch der Anorganischem Chemie*; Springer: Berlin, 1974, Vol. 14A, 1977, Vol. 49A, 1978, Vol. 50A. (b) Rosenblum, M. *Chemistry of the Iron Group Metallocenes*; Wiley: New York, 1965. (c) Coates, G. E.; Green, M. L. H.; Wade, K. *Organometallic Compounds*; Methuen: London, 1960; Vol. 2.
(3) (a) Saji, T.; Kinoshita, I. *J. Chem. Soc., Chem. Commun.* **1986**, 716. (b) Neuse, E. W.; Meirim, M. G.; Blom, N. F. *Organometallics* **1988**, *7*, 2562. (c) Beer, P. D. *Chem. Soc. Rev.* **1989**, *18*, 409. (d) Hall, C. D.; Danks, I. P.; Sharpe, N. W. *J. Organomet. Chem.* **1990**, *390*, 227. (e) Beer, P. D.; Sikanyika, H. *Polyhedron* **1990**, *9*, 1091. (f) Hall, C. D.; Tucker, J. H. R.; Sharpe, N. W. *Organometallics* **1991**, *10*, 1727. (g) Beer, P. D.; Tite, E. L.; Ibbotson, A. *J. Chem. Soc., Dalton Trans.* **1991**, 1691. (h) Medina, J. C.; Gay, I.; Chen, Z.; Echengoyen, L.; Gokel, G. W. *J. Am. Chem. Soc.* **1991**, *113*, 365. (i) Medina, J. C.; Li, C.; Bott, S. G.; Atwood, J. L.; Gokel, G. W. *J. Am. Chem. Soc.* **1991**, *113*, 366. (j) Constable, F. *Angew. Chem., Int. Ed. Engl.* **1991**, *30*, 407.
(4) Astruc, D.; Hamon, J. R.; Althoff, G.; Román, E.; Batail, P.; Michaud, P.; Mariot, J. P.; Varret, F.; Cozak, D. *J. Am. Chem. Soc.* **1979**, *101*, 5445.
(5) (a) Andrieux, C. P.; Blocman, C.; Dumas-Bouchiat, J. M.; M'Halla, F.; Savéant, J. M. *J. Am. Chem. Soc.* **1980**, *102*, 3806. (b) Andrieux, C. P.; Blocman, C.; Dumas-Bouchiat, J. M.; Savéant, J. M. *J. Am. Chem. Soc.* **1979**, *101*, 3431. (c) Guerchais, V.; Román, E.; Astruc, D. *Organometallics* **1986**, *5*, 2505.
(6) Astruc, D. *New J. Chem.* **1992**, *16*, 305.
(7) Grätzel, M., Ed. *Energy Resources Through Photochemistry and Catalysis*; Academic Press: New York, 1983.
(8) Osman, A. M.; El-Maghraby, M. A.; Hassan, Kh. M. *Bull. Chem. Soc. Jpn.* **1975**, *48*, 2226.
(9) Herberhold, M.; Ellinger, M.; Kremnitz, W. *J. Organomet. Chem.* **1983**, *241*, 227.
(10) Herberhold, M.; Ellinger, M.; Haumaier, L. *Organometallic Synthesis*; King, R. B., Eisch, Eds.; Elsevier: Amsterdam, 1986; Vol. 3, pp 81–83.
(11) Cullen, W. R.; Woolins, J. D. *Coord. Chem. Rev.* **1981**, *39*, 1.
(12) (a) Bracci, M.; Ercolani, C.; Floris, B.; Bassetti, M.; Chiesi-Villa, A.; Guastini, C. *J. Chem. Soc., Dalton Trans.* **1990**, 1357. (b) Chambron, J. C.; Coudret, C.; Sauvage, J. P. *New J. Chem.* **1992**, *16*, 361.
(13) Epstein, J. A.; Miller, J. S. In *Magnetic Molecular Materials*; Gatteschi, D., Kahn, O., Miller, J. S., Palacio, F., Eds.; NATO ASI Series No. 198; Kluwer: Dordrecht, The Netherlands, 1990; pp 151, 159.

0020-1669/93/1332-1197$04.00/0

spectroscopic characterization of the ligand *N,N'*-ethylenebis((ferrocenylmethylidene)amine), (η^5-C_5H_5)Fe[(η^5-C_5H_4)CH=N(CH_2)$_2$N=CH(η^5-C_5H_4)]Fe(η^5-C_5H_5) (**1**), its related amine (η^5-C_5H_5)Fe[(η^5-C_5H_4)CH_2NH(CH_2)$_2$NHCH_2(η^5-C_5H_4)]Fe(η^5-C_5H_5) (Fc_2L) (**2**), and the pentanuclear complex [Cu(Fc_2-L)$_2$(NO_3)$_2$]·2CH_3OH (**3**). The molecular and electronic structure and redox properties of **3** have been investigated by single-crystal X-ray diffraction, IR and EPR spectroscopies, variable-temperature magnetic susceptibility measurements, and cyclic voltammetry. The complex ability of **2** toward H^+ and Cu^{2+} has been investigated by potentiometry in dimethyl sulfoxide (dmso)–water mixtures.

Experimental Section

Reagents and Solvents. Ferrocenecarboxaldehyde, ethylenediamine, lithium aluminum borohydride, copper nitrate trihydrate and copper perchlorate hexahydrate were of reagent quality. They were obtained from commercial sources and used without further purification. The salt tetra-*n*-butylammonium hexafluorophosphate, [*n*-Bu_4N][PF_6], was recrystallized from ethanolic solution and dried at 80 °C under vacuum for 48 h. It was used as supporting electrolyte in the electrochemical experiments. Tetrahydrofuran and dichloromethane used were freshly distilled from sodium benzophenone and anhydrous $CaCl_2$, respectively. Benzene and isooctane were used as received. Dimethyl sulfoxide (dmso) was purified as previously described.[14] From this solvent, the dmso–water (80:20 w/w) mixture was easily prepared and used as solvent in the potentiometric study. Carbonate-free potassium hydroxide (0.08 mol dm^{-3}) and perchloric acid (0.1 mol dm^{-3}) solutions were used in the potentiometric experiments. Potassium perchlorate (0.1 mol dm^{-3}) was used as supporting electrolyte in this solvent mixture. Elemental analysis (C, H, N) were performed by the Servicio de Microanálisis Elemental de la Universidad Autónoma de Madrid (Spain).

Preparation of Compounds. *N,N'*-Ethylenebis((ferrocenylmethylidene)amine) (1). A mixture of ferrocenecarboxaldehyde, (η^5-C_5H_5)Fe(η^5-C_5H_4CHO), (856 mg, 4 mmol) and ethylenediamine (0.15 ml, 2 mmol) was refluxed for 1 h in benzene (50 mL) under argon atmosphere. The resulting yellow solution was evaporated to dryness and the oil residue was recrystallized from CH_2Cl_2/isooctane. The yellow solid (**1**) obtained was washed with isooctane and dried under vacuum. (850 mg, yield 70%). Anal. Calcd for $C_{24}H_{24}N_2Fe_2$ (**1**): C, 63.7; H, 5.3; N, 6.2. Found: C, 63.5; H, 5.5; N, 6.5. Infrared spectrum: 3095w, 3060w, 2950w, 2890w, 2820m, 1635s, 1465w, 1430w, 1405w, 1375m, 1348w, 1320m, 1280m, 1240m, 1210w, 1190w, 1110w, 1100s, 1060w, 1042m, 1010m, 1000m, 960w, 930w, 840w, 818s, 760w, 640w. ^{1}H NMR ($CDCl_3$) spectrum (in ppm): 3.79 (CH_2, 4H, s), 4.17 (C_5H_5, 10H, s), 4.36 (C_5H_5, 4H, s), 4.64 (C_5H_5, 4H, s), 8.19 (CH, 2H, s). ^{13}C NMR ($CDCl_3$) spectrum (in ppm): 62.14 (CH_2, s), 68.4 (C_5H_5, s), 69.08 (C_5H_5, s), 70.30 (C_5H_5, s), 80.41 (C_5H_5, s), 162.28 (CH, s).

***N,N'*-Ethylenebis((ferrocenylmethyl)amine) (2).** This ligand, Fc_2L, was obtained as follows: $LiAlH_4$ (152 mg, 4 mmol) was added to a tetrahydrofuran solution (50 mL) of **1** (940 mg, 2 mmol) under argon atmosphere. The resulting mixture was refluxed with stirring during 30 min. Small amounts of methanol were added in order to remove the excess of $LiAlH_4$. The suspension was filtered twice and the resulting pale yellow solution was evaporated to dryness under vacuum to yield an oil residue. **2** was obtained as a pale yellow solid by recrystallization of the oil from a CH_2Cl_2/isooctane mixtue (730 mg, yield 80%). Anal. Calcd for $C_{24}H_{28}N_2Fe_2$ (**2**): C, 63.2; H, 6.1; N, 6.1. Found: C, 62.9; H, 6.0; N, 5.9. Infrared spectrum: 3085w, 3060w, 2910w, 2890w, 2840w, 2825w, 1472w, 1459s, 1429w, 1405w, 1388w, 1370w, 1321m, 1256w, 1220m, 1152w, 1107s, 1100s, 1084m, 1048w, 1032m, 1021s, 998m, 920(w), 902w, 860w, 845m, 811s, 770s, 710m. ^{1}H NMR ($CDCl_3$) spectrum (in ppm): 1.85 (NH, 2H, broad signal), 2.72 (CH_2, 4H, s), 3.47 (CH_2, 4H, s), 4.07 (C_5H_5, 4H, s), 4.10 (C_5H_5, 10H, s), 4,14 (C_5H_5, 4H, s). ^{13}C NMR ($CDCl_3$) spectrum (in ppm): 48.73 (CH_2, s), 67.64 (C_5H_5, s), 68.32 (C_5H_5, s), 86.90 (C_5H_5, s).

Bis[*N,N'*-ethylenebis((ferrocenylmethyl)amine)]copper(II) Nitrate–Dimethanol (3). Copper(II) nitrate trihydrate (120 mg, 0.5 mmol) dissolved in a minimum amount of acetonitrile was added with stirring to an acetonitrile/methanol (1:3 v/v) solution of **2** (456 mg, 1 mmol). Yellow needles of **3** separated after 1 h. They were washed with methanol and dried under vacuum (415 mg, yield 80%). Anal. Calcd for $C_{50}H_{60}N_6O_8CuFe_4$ (**3**): C, 56.3; H, 4.7; N, 6.6. Found: C, 56.5; H, 4.6; N, 6.7. Infrared spectrum: 3440br,m, 3240m, 3170m, 3100m, 2940w, 2890w, 2430w, 1630w, 1470sh, 1445sh, 1380s, 1330w, 1230m, 1100m, 1040m, 1030w, 1000m, 950w, 920m, 820s, 750w, 525w, 485s, 360w. Single crystals of **3** suitable for X-ray diffraction were grown by slow diffusion between two CH_3CN/CH_3OH solutions containing **2** and copper(II) nitrate.

Physical Techniques. IR spectra were taken on a Perkin-Elmer 1750 spectrophotometer as KBr pellets. X-band powder EPR spectra were recorded with a ER 200D Brucker spectrometer equipped with a helium continuous-flow cryostat, a Hall probe and a frequency meter. NMR spectra were measured on a Brucker AC-200 FT spectrometer operating at 300 K. Chemical shifts for ^{1}H and ^{13}C{^{1}H} NMR spectra are referenced to TMS and $CDCl_3$. Magnetic measurements were carried out on polycrystalline samples in the 80–300 K temperature range with a previously described pendulum-type apparatus.[15] Electronic spectra were recorded on a Perkin-Elmer Lambda 9 spectrophotometer in solution and as Nujol mulls on filter paper. Cyclic voltammograms were obtained with a programmable function generator Tacusel IMT-1, connected to a Tacusel PJT 120-1 potentiostat. The working electrode was platinum, with a saturated calomel reference electrode separated from the test solution by a salt bridge containing the solvent/supporting electrolyte. The auxiliary electrode was platinum wire. The electrochemical cell used for controlled potential electrolysis was a conventional H-type design with separated anodic and cathodic compartments by a porous glass frit. The electrolysis was stopped when intensity was 1% of the initial, and the total charge was obtained by integration of the intensity/time curve. Tetrabutylammonium hexafluorophosphate and dichloromethane or dmso were used as supporting electrolyte and solvent respectively in the electrochemical experiments. The system was calibrated against ferrocene.

Potentiometric titrations were carried out in dmso–water (80:20 w/w) mixture at 25 °C, by using equipment (potentiometer, cell, buret, stirrer, microcomputer, etc.) that has been fully described.[16] The reference electrode was an Ag/AgCl electrode in saturated KCl solution. The glass electrode was dipped in dmso–water (80:20) for half an hour before use. It was calibrated as a hydrogen concentration probe by titration of well-known amounts of $HClO_4$ with CO_2-free NaOH solutions and determining the equivalent point by the Gran's method,[17] which gives the standard potential E^o, and the ionic product of water ($K'_w = [H^+][OH^-]$). The logarithm of K_w for the solvent used was found to be -18.34 ± 0.02 (25 °C, 0.1 mol dm^{-3} $KClO_4$). The concentration of the copper(II) solutions were determined gravimetrically by standard methods. The computer program SUPERQUAD[18] was used to calculate the protonation and stability constants. Solutions of **2** and copper(II) nitrate (c_{Fc_2L} = 10^{-3}–10^{-2} mol dm^{-3} and c_{Cu} = (1–5) × 10^{-3} mol dm^{-3} with c_{Fc_2L}/c_{Cu} = 2–4) previously acidified with $HClO_4$ were titrated with KOH to determine the protonation constants of Fc_2L and its complex formation.

Crystallographic Data Collection and Structure Determination. A well-shaped yellow needle of **3** with approximate dimensions 0.20 × 0.10 × 0.10 mm was mounted on a Enraf-Nonius CAD4 diffractometer and used for data collection. Intensity data were collected by using monochromatized Mo Kα radiation (λ = 0.710 73 Å). Unit cell dimensions were determined from the angular setting of 25 reflections with θ angles in the range 12–25°. A triclinic cell was obtained and the space group $P\bar{1}$ was confirmed from the structure determination. A summary of the crystallographic data and refinement results is given in Table I. Complete crystal data and experimental details are deposited as supplementary material (Table S1). A total of 4373 reflections were measured, *hkl* range 0,–13,–19 to 8,13,19 (0–25° θ range) using the ω–2θ scan technique, with a maximum scan time of 50 s per reflection. The intensity of three standard reflections monitored every 60 min showed no systematic variation. 2941 reflections were considered as observed with $I > 2.5\sigma(I)$. Lorentz and polarization corrections were applied but no allowance was made for absorption.

The positions of Cu, Fe(1) and Fe(2) atoms were determined from a Patterson interpretation. The remaining non-hydrogen atoms were located from successive difference electron density maps. The structure refinement was carried out by weighted full-matrix least-squares methods first

(14) Lloret, F.; Moratal, J.; Faus, J. *J. Chem. Soc., Dalton Trans.* **1983**, 1743.

(15) Bernier, J. C.; Poix, P. *Actual. Chim.* **1978**, *2*, 7.

(16) García-España, E.; Ballester, M. J.; Lloret, F.; Moratal, J.; Faus, J. *J. Chem. Soc., Dalton Trans.* **1988**, 101.

(17) Gran, G. *Analyst (London)* **1952**, *77*, 661. Rossotti, F. J.; Rossotti, H. J. *J. Chem. Educ.* **1965**, *42*, 375.

(18) Gans, P.; Sabatini, A.; Vacca, A. *J. Chem. Soc., Dalton Trans.* **1985**, 1195.

Table I. Crystallographic Data for $[CuL_2(NO_3)_2]\cdot 2CH_3OH$ (**3**)

chem formula	$C_{50}H_{60}N_6O_8CuFe_4$	fw	1160.0
a, Å	7.520(1)	space group	$P\bar{1}$
b, Å	11.047(2)	T, °C	20
c, Å	16.186(5)	λ, Å	0.710 73
α, deg	101.93(2)	ρ_{calcd}, g cm^{-3}	1.54
β, deg	97.24(2)	μ, cm^{-1}	16.13
γ, deg	104.95(1)	R^a	0.046
V, Å^3	1247.9(5)	$R_w{}^b$	0.051
Z	1		

^{a} $R = \sum(|F_o| - |F_c|)/\sum|F_o|$. ^{b} $R_w = [\sum w(|F_o| - |F_c|)^2/\sum w|F_o|^2]^{1/2}$, $w = 1/(\sigma^2(F_o) + 0.00388(F_o)^2)$.

with isotropic and then with anisotropic temperature factors for all non-hydrogen atoms (348 parameters). A difference Fourier synthesis allowed the location of all hydrogen atoms and they were refined isotropically riding on their parent atom. The refinement converged at $R = 0.046$ and $R_w = 0.051$. The final difference Fourier map shows residual maxima and minima of 0.64 and −0.55 e Å^{-3}. The scattering factors for all atoms and anomalous dispersion corrections terms for Cu and Fe were taken from ref 19. The computer programs SHELX-76[20] and PARST[21] were used in the crystallographic calculations. The molecular illustration was drawn by the program ORTEP.[22] All calculations were done on a IBM-3090 at the Centro de Cálculo de la Universitat de València. Final atomic coordinates for non-hydrogen atoms and selected bond distances and angles are listed in Tables II and III, respectively. A full listing of atomic coordinates and equivalent displacement parameters (Table S2), bond lengths and angles (Table S3) along with tables of anisotropic displacement parameters (Table S4), hydrogen atom coordinates and isotropic displacement parameters (Table S5), least-squares planes (Table S6), and donor–acceptor contacts concerning the hydrogen bonding (Table S7) are available as supplementary material.

Results and Discussion

Description of the Structure of 3. The structure of this complex consists of centrosymmetric neutral $[Cu(Fc_2L)_2(NO_3)_2]$ units and methanol crystallization molecules. An ORTEP view of the $[Cu(Fc_2L)_2(NO_3)_2]$ unit and the crystal packing are depicted in Figure 1a,b, respectively.

The copper(II) ion is in a 4 + 2 surrounding. The four nearest neighbors, at about 2 Å, are the four nitrogen atoms N(1), N(2), N(1)^i and N(2)^i from the two diferrocenyl-containing groups (Fc_2L) which act as bidentate ligands through the ethylenediamine-nitrogen atoms. The two apical positions are occupied by oxygen atoms of two nitrate anions at greater distance (2.515(6) Å for Cu–O(1)). The four nitrogen atoms of the basal plane are planar and the copper atom lies in this plane. The short bond angle around the copper atom in the five-membered ring (84.6(2)° for N(1)–Cu–N(2)) is due to the geometrical constraints in the coordinated ethylenediamine-type ligands. The CuN(1)C(2)C(3)N(2) ring adopts the usual chair conformation (the torsional angle N(1)–C(2)–C(3)–N(2) is 53.9(6)°). Bond distances and angles within this fragment are in agreement with those reported for other bis(*N*,*N*′-dialkylethylenediamine)copper(II) complexes.[23-25] No important distortions are present in the Fc_2L ligand, except perhaps the angle Cu–N(1)–C(1), 121.9(4)°, the main deviation found from an ideal geometry. The geometry of the Fc_2L ligand can be adequately described by the examination of the torsion angles: C(2)–C(3)–N(2)–C(4), C(3)–C(2)–N(1)–C(1), C(2)–N(1)–C(1)–C(10), C(3)–N(2)–C(4)–C(20), (88.2(6)°, 178.1(5)°, 66.7(6)°, and 70.3(6)°, respectively) and the dihedral angle between the C(10)–C(14) and C(20)–C(24) planes (106.7(3)°). The cyclopentadienyl groups are planar within the limits of experimental errors. The dihedral angle between the planes C(10)–C(14) and C(15)–C(19) at Fe(1) is 1.4(3)° and it is only 0.7(3)° in the other ferrocenyl fragment at Fe(2). The Fe(1) atom is at 1.647(2) Å and 1.645(2) Å from

Table II. Final Atomic Fractional Coordinates and Thermal Parameters[a,b] for Compound **3**

atom	x/a	y/b	z/c	B_{eq}, Å^2
Cu	0.0	0.0	0.5	2.10(3)
Fe(1)	0.4509(1)	0.2591(1)	0.8715(1)	2.84(3)
Fe(2)	0.0455(1)	0.2671(1)	0.2098(1)	2.89(3)
N(1)	0.1054(6)	0.1459(4)	0.6093(3)	2.2(1)
N(2)	−0.0610(6)	0.1410(4)	0.4464(3)	2.3(1)
N(3)	0.3719(6)	0.0142(5)	0.3986(3)	3.3(1)
C(1)	0.2693(8)	0.1489(6)	0.6736(3)	2.8(1)
C(2)	0.1329(8)	0.2685(6)	0.5835(4)	2.9(2)
C(3)	−0.0350(8)	0.2563(5)	0.5165(3)	2.6(2)
C(4)	0.0501(8)	0.1706(6)	0.3788(3)	2.6(2)
C(10)	0.2885(7)	0.2422(6)	0.7567(3)	2.7(1)
C(11)	0.4160(8)	0.3697(6)	0.7879(4)	3.4(2)
C(12)	0.3815(9)	0.4254(6)	0.8687(4)	3.7(2)
C(13)	0.2338(9)	0.3360(7)	0.8883(4)	3.9(2)
C(14)	0.1744(8)	0.2222(6)	0.8193(4)	3.3(2)
C(15)	0.596(1)	0.1267(8)	0.8505(5)	4.9(3)
C(16)	0.721(1)	0.2528(9)	0.8812(5)	5.6(3)
C(17)	0.682(1)	0.3047(9)	0.9642(5)	5.7(3)
C(18)	0.537(1)	0.2118(9)	0.9816(4)	5.4(3)
C(19)	0.484(1)	0.1016(8)	0.9127(5)	5.1(3)
C(20)	−0.0217(8)	−0.2506(6)	0.3256(3)	3.0(1)
C(21)	0.066(1)	0.3830(7)	0.3291(4)	4.2(2)
C(22)	−0.048(1)	0.4176(9)	0.2655(5)	5.2(3)
C(23)	−0.199(1)	0.310(1)	0.2238(5)	5.6(3)
C(24)	−0.1869(9)	0.2027(8)	0.2595(4)	4.6(2)
C(25)	0.237(1)	0.1698(7)	0.1866(5)	4.4(3)
C(26)	0.3109(9)	0.3002(7)	0.1846(4)	4.2(2)
C(27)	0.192(1)	0.3246(8)	0.1205(4)	4.4(2)
C(28)	0.046(1)	0.2117(8)	0.0814(4)	4.7(3)
C(29)	0.074(1)	0.1136(7)	0.1222(5)	4.6(2)
C(30)	0.6101(7)	0.4009(3)	0.4302(4)	6.2(3)
O(1)	0.3269(7)	0.0480(3)	0.4690(4)	3.5(1)
O(2)	0.5137(7)	0.0834(3)	0.3801(4)	4.1(2)
O(3)	0.2746(7)	−0.0864(3)	0.3456(4)	5.5(2)
O(4)	0.5474(7)	0.3372(3)	0.4935(4)	7.1(2)

^{a} Estimated standard deviations in the last significant digits, as observed from the least-squares refinement, are given in parentheses. ^{b} B values for anisotropically refined atoms are given in the form of the equivalent isotropic displacement parameter defined as $B_{eq} = {}^1/_3\sum_i\sum_j B_{ij}a_ia_j$.

Table III. Selected Bond Distances (Å) and Angles (deg) for **3**[a]

		Distances	
Cu–N(1)	2.041(4)	Cu–N(2)	2.053(5)
Cu–O(1)	2.515(6)	Fe(1)–C(10)	2.036(5)
Fe(1)–C(11)	2.038(7)	Fe(1)–C(12)	2.043(7)
Fe(1)–C(13)	2.048(8)	Fe(1)–C(14)	2.045(6)
Fe(1)–C(15)	2.041(9)	Fe(1)–C(16)	2.038(8)
Fe(1)–C(17)	2.026(8)	Fe(1)–C(18)	2.035(8)
Fe(1)–C(19)	2.048(9)	Fe(2)–C(20)	2.033(6)
Fe(2)–C(21)	2.048(6)	Fe(2)–C(22)	2.05(1)
Fe(2)–C(23)	2.04(1)	Fe(2)–C(24)	2.039(6)
Fe(2)–C(25)	2.035(9)	Fe(2)–C(26)	2.043(7)
Fe(2)–C(27)	2.031(8)	Fe(2)–C(28)	2.042(7)
Fe(2)–C(29)	2.051(8)	N(1)–C(1)	1.498(7)
N(1)–C(2)	1.471(8)	C(1)–C(10)	1.481(7)
C(2)–C(3)	1.515(8)	C(3)–N(2)	1.472(6)
N(2)–C(4)	1.497(8)	C(4)–C(20)	1.503(9)
		Angles	
O(1)–Cu–N(1)	87.1(2)	O(1)–Cu–N(2)	93.3(2)
N(1)–Cu–N(2)	84.6(2)	N(1)–Cu–N(2)^i	95.4(2)
C(10)–C(1)–N(1)	111.8(5)	Cu–N(1)–C(1)	121.9(4)
Cu–N(1)–C(2)	107.1(4)	C(1)–N(1)–C(2)	111.8(5)
N(1)–C(2)–C(3)	108.6(5)	C(2)–C(3)–N(2)	108.4(5)
Cu–N(2)–C(3)	108.0(3)	Cu–N(2)–C(4)	113.3(4)
C(3)–N(2)–C(4)	112.3(5)	N(2)–C(4)–C(20)	113.9(5)

[a] Roman numeral superscript refers to the following equivalent position relative to x, y, z: (i) $-x$, $-y$, $-z + 1$.

(19) Cromer, D. T.; Waber, T. *International Tables for X-ray Crystallography*; Kynoch Press: Birmingham, England, 1974; Vol. IV, p 99 (Table 2.2B).
(20) Sheldrick, G. M. SHELX-76. Program for crystal structure determination. University Chemical Laboratory, Cambridge, England, 1976.
(21) Nardelli, M. *Comput. Chem.* **1983**, *7*, 95.
(22) Johnson, C. K. *ORTEP*; Report ORNL-3794; Oak Ridge National Laboratory: Oak Ridge, TN, 1965.
(23) Korvenranta, J.; Pajunen, A. *Suom. Kemistil.* **1970**, *B43*, 119.
(24) Pajunen, A.; Korvenranta, J. *Suom. Kemistil.* **1973**, *B46*, 139.
(25) Korvenranta, J. *Suom. Kemistil.* **1973**, *B46*, 296.

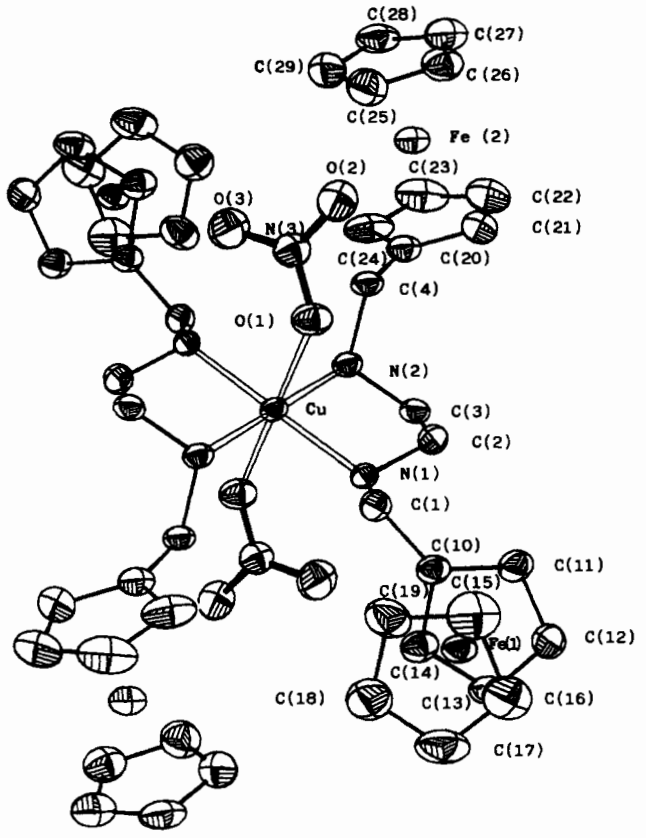

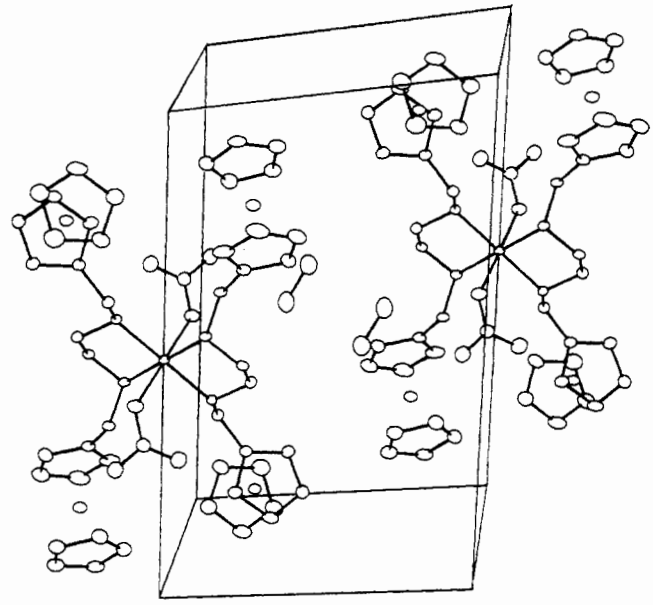

Figure 1. (a) Top: ORTEP drawing of $[Cu(Fc_2L)_2(NO_3)_2]$ complex with the atom-numbering scheme. Thermal ellipsoids are ploted at the 30% probability level. Hydrogen atoms and methanol molecules were omitted for clarity. (b) Bottom: View of the crystal packing down the *b*-axis. (The *c*-axis is vertical.)

the C(10)–C(14) and C(15)–C(19) planes, respectively (1.645(2) and 1.651(2) Å for Fe(2) respect to the C(20)–C(24) and C(25)–C(29) planes). Fe–C(cyclopentadienyl ring) distances range from 2.026(8) to 2.051(8) Å (av 2.04 Å) and intracyclopentadienyl C–C bond lengths lie in the range 1.39(1)–1.44(1) Å (av 1.42 Å), the geometry of the ferrocenyl fragments being very similar to that observed in ferrocene itself. The ferrocenyl groups are in an eclipsed conformation with twisting angles of 1.6(7) and 4.5(7)° at Fe(1) and Fe(2), respectively.[26] It is well-known that in the solid state ferrocene derivatives adopt both conformations, eclipsed or staggered, the occurrence of one particular conformation being most likely the result of packing forces. In fact, ab initio calculations on eclipsed and staggered conformations of cyclopentadienyl rings of ferrocene showed that the energy is essentially the same for both cases.[27]

The geometry of the nitrate anion is as expected. The N–O bond lengths and the intra-anion angles average 1.243 Å and 120°, respectively. O(2) and O(3) oxygen atoms contribute to the packing by forming hydrogen bonds with methanol molecules and amino groups. The donor–acceptor contacts concerning the hydrogen bonding are listed in Table S7 (supplementary material). The intramolecular Fe(1)···Cu and Fe(2)···Cu distances are 6.211(2) and 6.042(2) Å, respectively, values which exclude any significant direct interaction. The shortest intermolecular Cu···Cu^{ii} separation is 7.520(1) Å (where ii denotes the following equivalent coordinates: $x-1, y, z$; $-x-1, -y, -z+1$; $x+1, y, z$; $-x+1, -y, -z+1$).

Scheme I

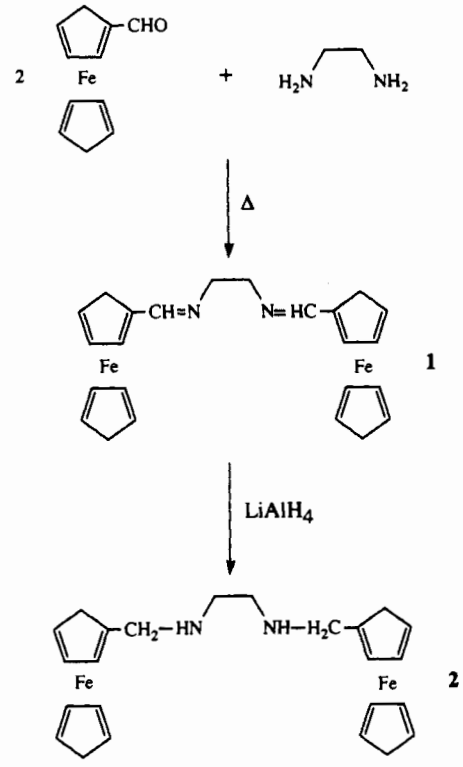

Synthesis of 1-3. The synthesis of ferrocene-containing ligands can be carried out by means of a wide variety of reactions depending on the starting ferrocenyl group. For instance, Schiff-base ferrocenyl-containing groups can be obtained by reaction of ferrocenylamine with an appropriate aldehyde[12] or with ferrocenecarboxaldehyde and appropriate amines.[3b] Nevertheless, the stability of the resulting imines toward hydrolysis is a problem for using them as ligands. In order to avoid it one can hydrogenate imines to yield the parent amines which would be much more stable in solution. The well-known bidentate ethylenediamine (en) ligand has been used as starting material together with ferrocenecarboxaldehyde to yield the Schiff-base complex **1** (see Scheme I).

Analytical and spectroscopic data are in agreement with the proposed formulation for **1**. ^{13}C NMR spectra of this compound reveals that the carbon atoms from the nonsubstituted cyclopentadienyl ring are equivalent (69.08 ppm) whereas the other three carbon NMR signals (68.40, 70.30 and 80.41 ppm) would be ascribed to the different carbon atoms in the substituted

(26) These angles are calculated as average of the dihedral angle defined as (cyclopentadienyl-C)–(centroid)–(centroid)–(cyclopentadienyl-C).

(27) Bagus, P. S.; Walgren, U. I.; Almlof, J. *J. Chem. Phys.* **1976**, *64*, 2324.

cyclopentadienyl ring. Signals at 62.14 and 162.28 ppm correspond to the CH_2 and CH carbon resonances, respectively. The hydrogenation of **1** by reaction with $LiAlH_4$ in freshly distilled THF (see Scheme I) yields the corresponding amine ligand **2**. Its IR spectrum shows several peaks corresponding to the ν(N–H) stretching vibration in the region 3300–3100 cm^{-1}. Furthermore, the ν(C=N) imine stretching peak which occurs as a strong absorption at 1630 cm^{-1} in the spectrum of **1**, is lacking for **2** as expected. The ^{13}C NMR spectrum of **2** exhibits three signals for the cyclopentadienyl rings, one of them appearing at lower field (86.90 ppm) indicating the ipso carbon resonance. The remaining two signals are ascribed to the nonsubstituted ring (68.32 ppm) and the substituted (68.32 and 67.64 ppm) rings.

The synthesis of compounds **1** and **2** was reported elsewhere[3b] but we have prepared them by a somewhat different method (see Experimental Section). They can be easily prepared as oils being very difficult to obtain them as solids. The use of CH_2Cl_2/isooctane to crystallize **1** and **2** provide us with pure solids. **1** and **2** can also be obtained as ground materials with repeating washing of the oil with hexane or isooctane and solvent elimination under vacuum to dryness. The yellow solids so obtained have a lower purity but they can be prepared in high yield and as such can be used for synthetic purposes. **2** was obtained in a very high purity (for potentiometric studies) as follows: addition of *p*-toluenesulfonic acid to an acetone solution of **2** yields a brown-yellowish solid (the corresponding protonated diamine *p*-toluenesulfonate salt) which was filtered off and dried under reduced pressure. It was dissolved in water and high-purity **2** was precipitated as a crystalline yellow solid by neutralization with sodium bicarbonate. This solid was filtered off, washed with water, and dried under vacuum.

Both compounds **1** and **2** are potential N-donor bidentate ferrocenyl-containing ligands. It seemed us very interesting to check their chelating capability toward metal ions and analyze the influence of the bulky ferrocenyl groups near the coordination sites. Preliminary studies with **1** show that the imine group is unstable in solution due to the hydrolytic reaction in the presence of water or metal ions. However, the parent amine **2** is much more stable and its solutions do not exhibit any sign of decomposition. The low solubility of **2** in water and water/methanol or water/dioxane mixtures preclude their use as solvents for the potentiometric investigations. The high solubility of **2** in dmso led us to use a water/dmso mixture to investigate its affinity toward H^+ and metal ions (vide infra). The synthesis of **3** and its X-ray data show unequivocally that **2** can act as a chelating ligand. The most relevant features of the infrared spectrum of **3** are a broad band at 3440 cm^{-1} (O–H stretching of methanol), a doublet at 3240 and 3170 cm^{-1} (N–H stretching of amine) and a strong band at 1380 cm^{-1} (N–O stretching of nitrate). They are in agreement with the structural information.

Electronic Properties. Complexes **1–3** are stable crystalline solid materials. They are yellow, the origin of this color being the occurrence of a band centered at 430 nm in both reflectance and solution spectra. A very intense and sharp absorption at 250 nm is observed in the solution (dmso) spectra of **1** and **2**. In the case of **3**, this band exhibits a shoulder due to the absorption of nitrate. The d–d transitions of the central copper(II) ion in **3** are detectable as a shoulder near 570 nm and they are obscured by the intense absorptions at lower wavelengths. This latter absorption is in agreement with the elongated tetragonal octahedral CuN_4O_2 chromophore in **3**.[28]

The thermal variation of the molar susceptibility of **3** is depicted in Figure 2 as $1/\chi_M$ versus T. A Curie law is observed in the temperature range investigated (300–80 K) with a μ_{eff} value of 1.80 μ_B which is as expected for a $S = {}^1/_2$ system with $g = 2.08$. The X-band EPR spectrum of **3** recorded on a microcrystalline powder sample looks like a quasi isotropic axial doublet (see Figure 2) with an average g value of 2.07. It shows no significant variation from room temperature to 4.2 K. No half-field transition is observed in agreement with its monomeric nature.

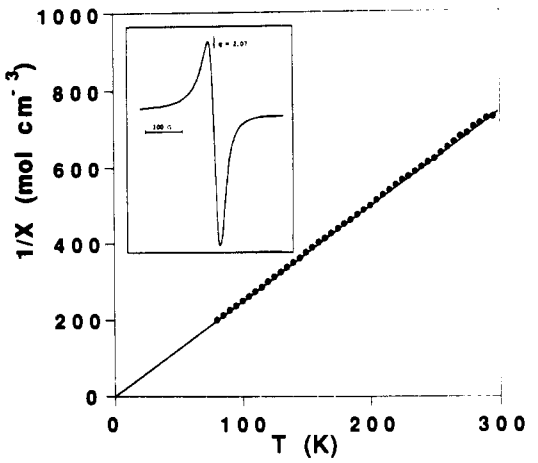

Figure 2. Thermal variation of the inverse of the molar magnetic susceptibility (χ_M) of **3** (solid line represents best fit to data) and X-band EPR spectrum of **3** at 4.2 K.

Table IV. Electrochemical Data[a]

compd	E_{pa},[b] V	E_{pc},[c] V	$10^3\Delta E_{pac}$,[d] V
1	0.60	0.52	82
2	0.45 (0.47)	0.37 (0.40)	80 (72)
3	(0.61)	(0.46)	(150)
ferrocene	0.46	0.38	77
ferrocenecarboxaldehyde	0.77	0.68	90

[a] Obtained in dichloromethane, 0.1 mol dm^{-3} [n-Bu_4N][PF_6] as supporting electrolyte. Values in parentheses were obtained in dmso. Potentials were determined with reference to the SCE. Scan rate 0.1 V s^{-1}. [b] Anodic peak potential. [c] Cathodic peak potential. [d] Difference between anodic and cathodic peak potentials.

Cyclic Voltammetry Study. The electrochemical behavior of compounds **1–3** has been investigated by cyclic voltammetry, a rotating disk electrode (RDE), and coulometry. Electrochemical experiments were carried out at room temperature in the presence of [n-Bu_4N][PF_6] as supporting electrolyte and using as solvent CH_2Cl_2 (**1** and **2**) and dmso (**2** and **3**). The electrochemical data are summarized in Table IV.

Compounds **1** and **2** show in CH_2Cl_2 only an oxidation peak (A) at 0.60 V (**1**) and 0.45 V (**2**) and the corresponding reduction peak (A′) is found if the sweep is reversed. The couple A/A′ is reversible with a separation peak of about 80 mV (ferrocene in the same conditions give an ΔEp of 77 mV) and with an anodic and cathodic intensities ratio close to the unity in both cases. Plots of i_d versus $w^{1/2}$ (from RDE experiences; i_d = diffusion intensity and w = angular velocity of rotating disk electrode) and i_p versus $v^{1/2}$ (from cyclic voltammetry experiences; i_p = anodic peak intensity and v = scan rate) indicate that the chemical oxidation is controlled by diffusion. Controlled-potential electrolysis and coulometry show that the final oxidation process was found after passage of 2 F/mol indicating that (in **1** and **2**) the two ferrocenyl moieties oxidize at the same potential. However the oxidation process would be better described as two monoelectronic processes occurring in the same molecule, taking into account the separation peak of 80 mV found which is the same obtained for the ferrocene standard compound (a bielectronic reversible process would have half the peak separation value compared to that found for ferrocene). This means that the organic framework attached to the ferrocenyl groups does not allow communication between the two centers and delocalization is not possible making the two moieties independent. Thus from an electrochemical point of view **1** and **2** can be described as

(28) Hathaway, B. J. *Struct. Bonding* **1984**, *57*, 55.

Table V. Equilibrium Data[a] for Basicity and Formation of Cu(II) Complexes with Fc_2L and en in dmso–water (80:20 w/w) (25 °C, 0.1 mol dm^{-3} $KClO_4$)

eq no.	reacn	log β
1	$Fc_2L + H^+ \leftrightarrow HFc_2L^+$	9.40(1)
2	$HFc_2L^+ + H^+ \leftrightarrow H_2Fc_2L^{2+}$	6.40(1)
3	$en + H^+ \leftrightarrow Hen^+$	10.00(1)[b]
4	$Hen^+ + H^+ \leftrightarrow H_2en^{2+}$	6.94(1)[b]
5	$Cu^{2+} + Fc_2L \leftrightarrow Cu(Fc_2L)^{2+}$	9.77(1)
6	$Cu(Fc_2L)^{2+} + Fc_2L \leftrightarrow Cu(Fc_2L)_2^{2+}$	6.23(5)
7	$2Cu^{2+} + 2Fc_2L + 2H_2O \leftrightarrow Cu_2(Fc_2L)_2(OH)_2^{2+} + 2H^+$	10.38(6)
8	$Cu^{2+} + en \leftrightarrow Cu(en)^{2+}$	11.02(1)[b]
9	$Cu(en)^{2+} + en \leftrightarrow Cu(en)_2^{2+}$	9.70(2)[b]

[a] Values in parentheses are the standard deviations in the last significant digits. [b] Values taken from ref 29.

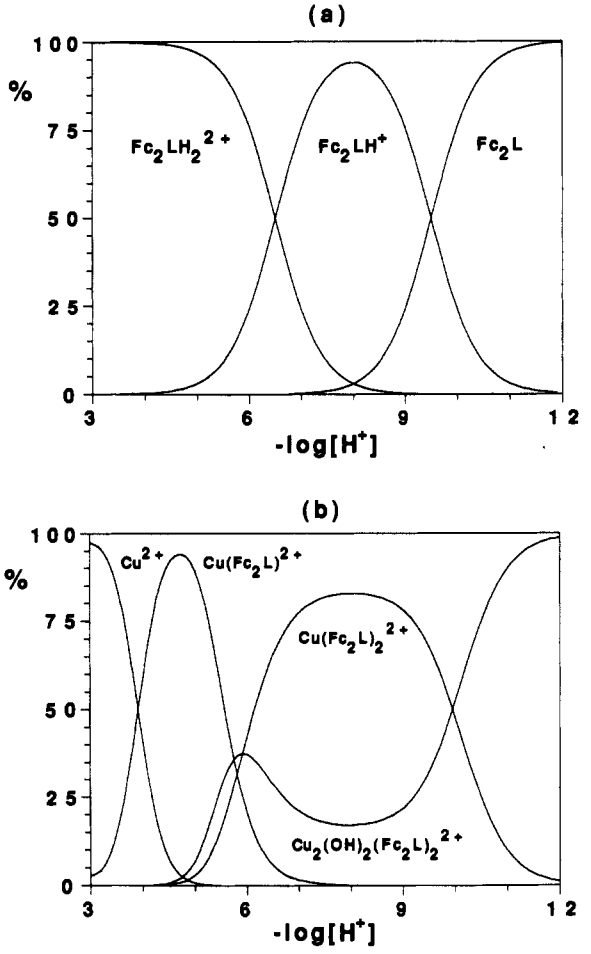

Figure 3. Distribution diagrams of the species in equilibrium for Fc_2L–H^+ (a) and Cu^{2+}–Fc_2L (b) systems as a function of pH (c_{Cu} = 5 × 10^{-3} mol dm^{-3}; c_{Fc_2L} = 1.5 × 10^{-2} mol dm^{-3}).

composed by two equal noninteracting monoelectronic redox groups that oxidize at the same potential.

After electrolysis in CH_2Cl_2, **2** shows a cathodic wave with $E_{1/2}$ potential values close to that found for the starting complex, indicating that the corresponding oxidized species could be obtained in this solvent. We are looking for adequate counterions to precipitate it in a crystalline form. This behavior contrasts with that of **1**, where no well-defined peaks were detected after electrolysis.

The electrochemical study of **3** was performed in dmso. The use of other common solvents was discarded because of its insolubility. This compound shows one-wave oxidation which shifted to greater anodic potentials with respect to the free ligand **2**. The change of the oxidation potential value of the ferrocene–ferrocenium couple could be due to the cationic nature of **3** versus

Scheme II

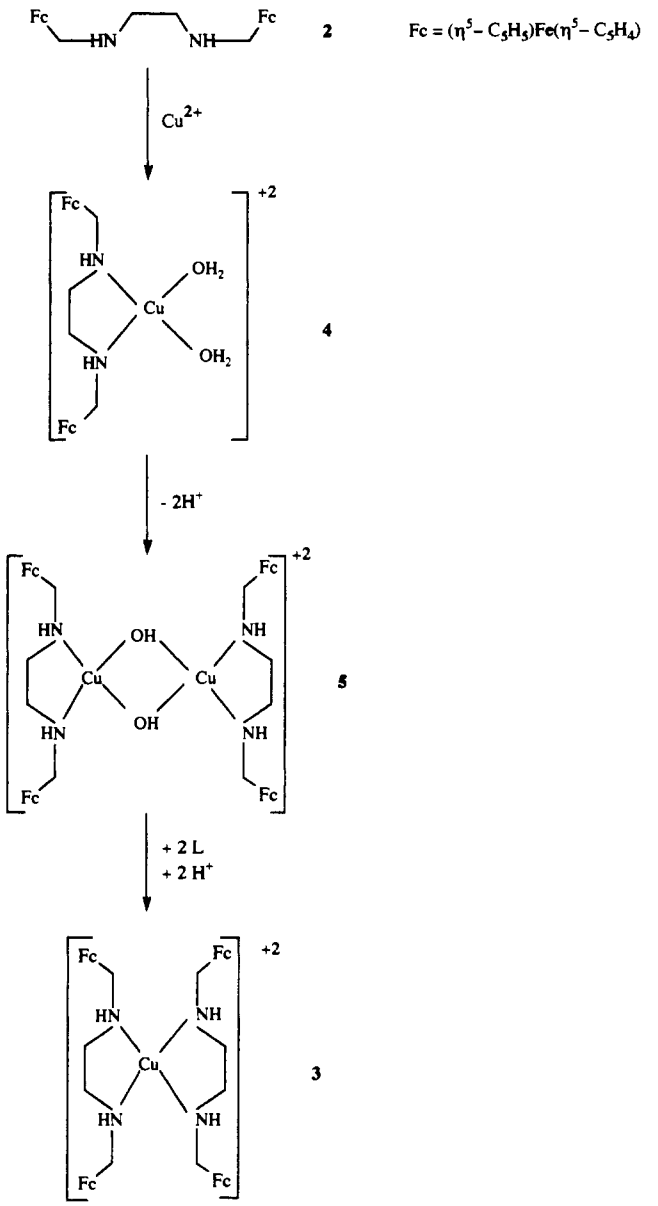

the neutral of **2** although the presence of metal coordinated atoms near the redox active centers could also be at the origin of this shift. However, for **3** the oxidation process appears not to be totally reversible bearing in mind the peak separation of 150 mV which is observed. On the other hand, plots of i_p versus $v^{1/2}$ and i_d versus $w^{1/2}$ are not linear indicating that the oxidation process is not controlled by diffusion. These data suggest that a chemical reaction is coupled with the electrochemical one. Controlled-potential electrolysis and coulometry were also carried out for **3** and the final oxidation process was found after passage of approximately 4 F/mol, a quantity which corresponds to the oxidation of the four ferrocenyl groups. After electrolysis, a cathodic wave assigned to free copper(II) was detected indicating that the corresponding oxidized species is unstable in these conditions.

For the sake of comparison, we have investigated the electrochemical behavior of **2** also in dmso. Cyclic voltammetry of **2** in this solvent shows an oxidation peak at 0.47 V (a value very close to that observed in CH_2Cl_2). Controlled-potential electrolysis was performed and the final oxidation process was found after passage of 1 F/mol. After electrolysis, cyclic voltammetry showed only one-reversible oxidation wave at 0.61 V. These data suggest that the oxidized species in dmso are unstable and a chemical–electrochemical reaction takes place to give a stable

Fe(II) compound that oxidizes at a high potential value. Further studies are in progress in order to isolate this complex related with the 0.6 V oxidation peak. These data indicate that the corresponding 2^{2+} species is unstable in dmso in contrast with its behavior found in CH_2Cl_2 probably also preventing the isolation of the oxidized form of **3**. Unfortunately, as discussed before, no solvent other than dmso can be used for **3**.

Potentiometric Study of the Fc_2L–Cu^{II}–H^+ System. The protonation of **2**, Fc_2L, and its complex formation with copper(II) was investigated by potentiometric titrations with KOH of previously acidified solutions of Fc_2L and Cu(II) for which c_{Fc_2L} and c_{Fc_2L}/c_{Cu} was varied in a wide range (see Experimental Section). Data processing by the SUPERQUAD program of 70 and 110 experimental points for the Fc_2L–H^+ and Fc_2L–H^+–Cu^{2+} systems, respectively, taken from different experiments for each system, allowed us to determine the corresponding protonation and stability constants. The protonation of ethylenediamine and the Cu^{2+}–en stability constants were determined previously in the same conditions.[29] All these protonation and stability constants are gathered in Table V. The distribution diagrams of the $H_jFc_2L^{j+}$ and $[Cu_p(Fc_2L)_qH_r]^{(2p+r)}$ species are depicted in Figure 3. In the absence of copper(II) (Figure 3a) $H_2Fc_2L^{2+}$ and neutral Fc_2L species are the only existing ones in the more acidic (pH $\leq$ 5) and more basic (pH $\leq$ 11) regions, respectively. HFc_2L^+ coexists with them in the intermediate pH region, being the predominant species at pH = 8. The observed protonation constant of Fc_2L (eqs 1 and 2 in Table V) are close to those of en (eqs 3 and 4) under the same conditions, and consequently, the basic character of en remains practically unaffected by the insertion of ferrocenylmethyl substituents on the amine-nitrogen atoms. However, the presence of these bulky ferrocenyl groups can introduce steric effects in their metal complexes especially in those of higher stoichiometry. In this regard, the values of the logarithms of the stability constants of $[Cu(Fc_2L)]^{2+}$ (eq 5) and $[Cu(Fc_2L)_2]^{2+}$ (eq 6) are 1 and 3 orders of magnitude smaller than those of their parent $Cu(en)^{2+}$ (eq 8) and $Cu(en)_2^{2+}$ (eq 9) complexes, respectively. The steric effects of the ferrocenyl substituents are most likely at the origin of the loss of stability. Although the coordination of the first ligand, Fc_2L, to copper(II) would not cause significant steric hindrance, the introduction of the second Fc_2L group to yield the square-planar $[Cu(Fc_2L)_2]^{2+}$ complex is accompanied by geometrical constraints as shown by the relative positions of the ferrocenyl substituents in the structure of **3**. Along this line, the average copper–nitrogen bond length in **3** (2.05 Å) is somewhat greater than the reported one in the parent copper(II) complexes with *N,N'*-bis(methyl-substituted)ethylenediamine (2.00 Å).[23-25] However, given the square planar arrangement of four nitrogen atoms around the metal ion in **3**, it can be concluded that the steric effects in the present case are not so significant as to induce a tetrahedral distortion of the CuN_4 chromophore.

The loss of stability of the complex $[Cu(Fc_2L)_2]^{2+}$ is responsible for the occurrence of the (μ-dihydroxo)copper(II) complex $[Cu_2(Fc_2L)_2(OH)_2]^{2+}$. The probable lack of geometrical constraints in the species makes possible its simultaneous formation with $[Cu(Fc_2L)_2]^{2+}$. The fact that the formation of the parent hydroxo complex in the Cu^{2+}–en system has not been observed under the same conditions supports this assumption. Nevertheless, (μ-dihydroxo)copper(II) complexes containing chelating *N,N'*-(alkyl-substituted)ethylenediamine ligands as terminal groups have been characterized both in solution and in the solid state.[30,31] $Cu_2(Fc_2L)_2(OH)_2]^{2+}$ exists in a wide pH range (pH > 5) (Figure 3b), and its formation curve exhibits a maximum at pH = 6, whereas at higher pH values it first decreases and finally increases to become the only existing species at pH > 11. Such an irregular distribution diagram is due to the relative stability of the $[Cu(Fc_2L)_2]^{2+}$ and $[Cu_2(Fc_2L)_2(OH)_2]^{2+}$ complexes. The formation of the different existing species in solution is shown in Scheme II.

It deserves to be noted that only experimental data belonging to the pH range 2–8 were computed because of the precipitation of the $[Cu_2(Fc_2L)_2](ClO_4)_2$ complex as a blue powder at pH > 8. This complex redissolves slowly in a more basic media to yield most likely the μ-dihydroxo species $[Cu_2(Fc_2L)_2(OH)_2]^{2+}$. All our attempts to grow single crystals of this hydroxo species from such basic solutions (pH $\sim$ 11–12) have been unsuccessful.

Acknowledgment. This work was partially supported by the Comision Interministerial de Ciencia y Tecnología (Proyecto PB91-0807-C02). Thanks are due to the Servicio de Espectroscopía and to the Centro de Cálculo de la Universitat de València for instrumental and computing facilities, respectively.

Supplementary Material Available: Tables of crystal data, positional parameters, bond distances and angles, thermal parameters, and least-squares planes and dihedral angles (14 pages). Ordering information is given on any current masthead page.

(29) Lloret, F.; Mollar, M.; Faus, J.; Julve, M.; Castro, I.; Diaz, W. *Inorg. Chim. Acta* **1991**, *189*, 195.

(30) Gustafson, R. L.; Martell, A. E. *J. Am. Chem. Soc.* **1959**, *81*, 525.

(31) Hatfield, W. E. In *Magneto-Structural Correlations in Exchange Coupled Systems*; Gatteschi, D., Kahn, O., Willett, R. D., Eds.; NATO ASI Series No. 140; Reidel: Dorchecht, The Netherlands, 1985; p 555 and references therein.